7.0 Tesla MRI Brain Atlas

7.0 Tesla MRI Brain Atlas

Editor Zang-Hee Cho, Ph D

Neuroscience Research Institute
Gachon University of Medicine and Science
Incheon, Republic of Korea

Springer

Zang-Hee Cho, Ph D
Neuroscience Research Institute
Gachon University of Medicine and Science
Incheon, Republic of Korea
zcho@gachon.ac.kr

ISBN 978-1-60761-153-0 e-ISBN 978-1-60761-154-7
DOI 10.1007/978-1-60761-154-7
Springer New York Dordrecht Heidelberg London

Library of Congress Control Number: 2009931582

Printed on acid-free paper

Springer is part of Springer Science+Business Media (www.springer.com)

To Dr. Gil-Ya Lee,
Founder of the Neuroscience Research Institute,
Gachon University of Medicine and Science

7.0 Tesla MRI Brain Atlas

Ultra-High Resolution Human Brain Maps Obtained by 7.0T MRI *In Vivo* and Cadaver Cryomacrotome, Based on a New Reference System

7.0T MRI Imaging

** Zang-Hee Cho, Ph.D[1,8]
Young-Bo Kim, MD, Ph.D[1]
Jae-Yong Han, Ph.D[1]
Hoon-Ki Min, M.Sc.[1,8]
Sang-Han Choi, M.Sc.[1]

Cryomacrotome Imaging

* Min Suk Chung, MD, Ph.D[2]
Jin Seo Park, Ph.D[5]
Jun-Won Lee, B.S.[2]
Hyo Seok Park, B.S.[5]
Dong Sun Shin Ph.D[2]
Dong-Hwan Har, Ph.D[6]
Do-Hee Cho M.Sc.[6]

Neuroanatomy

* Je-Geun Chi, MD, Ph.D[3]
Chan-Woong Park, MD, Ph.D[1]
Cheol-Wan Park, MD, Ph.D[1]
Young-Bo Kim, MD, Ph.D[1]
Jong-Min Lee, Ph.D[7]
James H. Fallon, Ph.D[8]

Neurology

* Duk L. Na, MD, Ph.D[4]
So-Young Moon, MD[2]
Sang Won Seo, MD[4]
Sook-Hui Kim, MD[4]
Seok-Min Go, MD[4]

** Principal Author

* Co-principal Authors

1 Neuroscience Research Institute (NRI), Gachon University of Medicine and Science, Incheon, Republic of Korea

2 Department of Anatomy, Ajou University School of Medicine, Suwon, Republic of Korea

3 Seoul National University College of Medicine, Seoul, Republic of Korea

4 Department of Neurology, Samsung Medical Center, Sungkyunkwan University School of Medicine, Seoul, Republic of Korea

5 Department of Anatomy, Dongguk University College of Medicine, Gyeongju, Republic of Korea

6 Graduate School of Advanced Imaging Science, Multimedia & Film, Chung-Ang University, Seoul, Republic of Korea

7 Department of Biomedical Engineering, Hanyang University, Seoul, Republic of Korea

8 University of California, Irvine, School of Medicine, Irvine, CA, USA

Foreword

I write this foreword in gratitude to Professor Zang-Hee Cho, one of the greatest innovators and proponents of progress in the field of magnetic resonance imaging. The *7.0 Telsa MRI Brain Atlas* prepared by Professor Cho and his colleague at the Neuroscience Research Institute, Gachon University of Medicine and Science will set new standards in the field of neuroanatomy. It is indeed fascinating to browse through this atlas that has been produced using both cadaver macrotome and images obtained using 7.0 Tesla (T) magnetic resonance imaging (MRI). This volume illustrates the considerable sensitivity and applicability of modern MRI that has been developed and perfected over the past decades by numerous scientists and engineers around the world. The research group of Professor Zang-Hee Cho was instrumental in rendering these astounding developments possible.

On careful study, the photographs provided in the Atlas reveal a wealth of information on the brain stem and midbrain structures, the *in vivo* visualization of which were once considered to be impossible. I am convinced that these remarkable achievements are a triumph of modern advanced MRI and of medical technology as a whole. MRI has already been demonstrated to be very helpful for the localization of early tumors and has been shown to provide timely information on the possibility of strokes and spinal cord degeneration. MRI is now entering into a new era in the field of brain imaging by enabling the detection of hippocampal deformations and atrophy; these conditions of the hippocampus are considered to be the main causes of Alzheimer's disease and epilepsy by many experts. Modern ultra-high-field (UHF) MRI investigations are not only capable of imaging the minute details of the above mentioned deformations and atrophy of the hippocampus but can also help distinguish between the normal and abnormal neuromorphology of the substantia nigra, which is the key neuronal site associated with major movement disorders such as Parkinson's disease. In addition to its use in the detection of deformities in the fine structures of the brain—the most intricate organ of our human body—this technique can be used for determining the target sites of therapeutic agents, including the subthalamic nucleus and globus pallidus; such a determination was previously considered impossible *in vivo.* This advantage of UHF MRI has facilitated deep brain stimulation (DBS) surgery. Currently, it is possible to rely on the cadaver brain atlas and apply computer-fitting to low-resolution MRI or computed tomography (CT) images, by taking advantage of microelectrode molecular probes. The same procedure could be applied *in vivo* in the field of submillimeter precision neuroanatomy.

Significant analogy could be considered to be present between discoveries by astronomical telescopes and the developments in the fields of medicine and biology. Previously unknown galaxies are discovered with each step of improvement in astronomical telescope resolution similarly, new revelations are made in the fields of medicine and biology with improvement in instruments. Especially in the field of brain science, numerous discoveries are still to be made and further interpretation and understanding of the associated mechanisms at the macroscopic and morphological level as well as on the biomolecular and cellular grounds are required. Magnetic resonance studies, especially those involving UHF MRI, will continue to play a fundamental role in this field. I am convinced that the *7.0 Telsa MRI Brain Atlas* will provide many answers and inspiration for further experimental studies. Thus, it can be considered to be a very valuable addition to any reputed library of medicine and an inexhaustible source of information for specialists and students.

Zurich, September 9, 2008

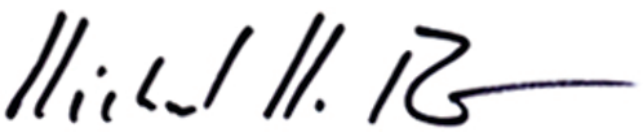

Laboratorium für Physikalische Chemie
Wolfgang-Pauli-Strasse 10, HCI D217
8093 Zürich, Switzerland

*Professor Ernst received the Nobel Prize in Chemistry in 1991 for his contribution to the development of Fourier Transform NMR, which not only revolutionized modern NMR but is also the backbone of MRI, magnetic resonance imaging, to which mankind owes so much today.

Preface

As is the case in any scientific field, advances in neuroanatomy have been enabled by the improvement in the tools available to researchers. These tools have undergone revolutionary changes in the past 100 years. When one of the first Nobel Prizes in the field of neuroscience was awarded to Camillo Golgi and Santiago Ramon y Cajal in 1906, the main research technique available to neuroscientists was the visual or optical microscopic examination of stained nerve cells. When numerous forms of scanning electron microscopy were introduced in the 20th century, they were immediately applied to the field of neuroanatomy, which greatly benefited from this technological advancement.

Among the tools and techniques available for neuroanatomy research, the imaging techniques that allow the researcher to perform *in vivo* studies of the human brain play especially significant roles in the advancement of the field. These imaging techniques include CT scanning using X-rays, nuclear imaging techniques such as positron emission tomography (PET) and single-photon emission computed tomography (SPECT), and MRI. Recent advances in MRI, especially in the area of ultra-high-field (UHF) MRI such as 7.0 Tesla (T), have attracted significant attention in the field of brain imaging for neuroscience, as well as in clinical research. Several physical and engineering problems related to UHF MRI are yet to be resolved. For example, due to the increased radio frequency (RF) in UHF MRI, image distortions are formed as a consequence of RF field inhomogeneities. Nevertheless, with the drastically improved contrast and resolution offered by these images obtained with 7.0 T MRI, previously unseen images of numerous fine structures in the human brain have been revealed *in vivo*. These structures include the subthalamic nucleus, the substantia nigra and their surroundings in the midbrain region, as well as various abnormalities found in associated regions. Since these images began to reveal numerous strikingly fine structural details in the human brain *in vivo*, many experts in the field of neuroscience started pondering on how high resolution MRI would affect the fields of modern medicine and neuroscience research as a whole.

Interest in the advances in the field of neuroanatomy is no longer restricted to anatomists. In order to understand the functional concepts of the nervous system, comprehending its structural organization is essential. Therefore, gaining an in-depth understanding of the subtle details of brain structure became important to enable lucid communication amongst clinicians, scientists, and other specialists working in the field of neuroscience and clinical medicine. The wealth of information provided by modern imaging techniques makes it imperative for the interpreter of the images to be thoroughly familiar with the minutiae of brain anatomy. Specialized knowledge of brain anatomy is a prerequisite; this means that the interpreters should possess knowledge of the gross anatomy of the brain and also be completely familiar with brain sections in various planes. Currently, it is not adequate to describe brain structures vaguely with terms such as the “fronto-parietal region” or “basal ganglia.” It is also necessary to precisely define and describe the specific gyrus or nucleus involved in pathological processes.

New neuroimaging applications are reported almost on a daily basis. Previously, the determination of the location, extent, and exact position of an intracranial space-occupying lesion was considered to be significant. Presently, the goal of clinical studies has extended in such a manner that the definition of the non-neoplastic lesions, i.e., cerebral hemorrhage, edema, and infarction, as well as demyelinating diseases and various neurodegenerative processes, is also considered to be crucial.

Let us consider the following analogy. When a new generation of giant cosmic telescopes became available to astronomers, these new tools not only offered the advantage of increased resolution and clearer and more informative images, but also enabled them to gain a new level of understanding of the universe. Similarly, with improvements in the field strength and resolution in MR imaging, it became possible to acquire images with unprecedented resolution and contrast. In addition to the obvious signal-to-noise improvement predicted by the laws of physics, variations in MRI tissue physical parameters, such as T1 and T2 relaxation times or their combinations were observed. From another front, considerable advances in the

imaging of human cadavers using cryomacrotome with increased sophistication and improved techniques have allowed us to obtain cadaver images of unprecedented resolution and contrast with markedly conserved brain structures. With these high-resolution images obtained with UHF MRI and recent advances in cryomacrotome technology, we were of the opinion that the construction of a New Brain Atlas would be an important and timely contribution to the medical and neuroscience community.

Therefore, in this book, we prepared a set of ultra-high resolution brain images obtained from a cadaver using a cryomacrotome and reconstructed partner images (sagittal and coronal), together with corresponding *in vivo* ultra-high resolution human brain images obtained with 7.0 T MRI. Thus, we were able to obtain a complete set of images for the entire brain atlas with axial, sagittal, and coronal images of the cadaver and corresponding set of 7.0 T MRI images of the *in vivo* human brain. In this book, we applied a reference system that is applicable to both cadaver gross anatomy and MRI anatomy. In addition, a cartesian axis system is defined on the midpoint of central intercommissural distance, with coordinates expressed in mm and ± along axial, coronal, and sagittal planes. This system will enable us to standardize the sectional planes and the levels at which the slices were obtained in any brain that may be encountered during clinical practice.

We have also applied a reference-adjusted unit designed to enable the reader, i.e., the MRI user, to predict the structure from any plane, regardless of the absolute size of the image of the brain obtained with clinical MRI. We expect our image numbering system to contribute to the establishment of a clinicopathologic mapping system of the human brain through massive global feedback of related information. Eventually, we hope that this book will serve as a roadmap in both clinical and neuroscience research in the years to come.

Zang-Hee Cho
Min Suk Chung
Je-Geun Chi
Duk L. Na

Table of Contents

Introduction

Introduction

1. Reference for Brain Images

The cadaver brain used in this atlas was designated as the “reference” brain, because this brain was used as a reference to compare brain images obtained with *in vivo* human brain of 7.0 T MRI. However, note that the cadaver image does not represent the “standard” brain image. The slices are shown at 2 mm intervals from the zero point along the axial and coronal planes, and at ± 2 mm intervals from the center. In this image, the horizontal plane through the anterior commissure (AC) and posterior commissure (PC) line was asigned as the midline delineating the axial slice, and the plane perpendicular to the center point of the AC-PC line was asigned as the midline delineating the coronal slice. In the sagittal slices, both the cadaver and MRI images start at ±2 mm from the center point, with the AC-PC line being aligned as the midline.

Images of the cadaver (reference) brain were juxtaposed on 7.0 T MRI images of the brain of a living subject to compare the anatomy of the two brains. In each set of images, the cadaver (reference) brain image is placed on the left page while the corresponding MRI image is placed on the right page to facilitate comparison. We have attempted to match the MRI brain images as closely as possible with the cadaver images. This type of presentation will facilitate correlational visualization of the anatomy of the reference image with that of the corresponding MR image.

2. Orientation of Brain Images

i. Orientation of the image sections and planes

Though there are several common protocols for the orientation of cross-sectional images, no standard protocol has been established of yet. In fact, there has been a considerable amount of confusion regarding the manner in which axial images should be viewed. Currently in clinical practice, all coronal images are viewed as shown in Fig. 1 (i); this is the view that would be observed if the examiner and the patient viewed each other face-to-face. The left side of the coronal image is the right side of the subject, as if in a mirror image (See Fig. 1 (ii)). The axial view images are also shown as if the examiner viewed the head of the patient from the bottom.

This type of arrangement of axial, sagittal, and coronal view images has been widely adopted in recent years. Therefore, we will follow this convention in our *7.0 Telsa MRI Brain Atlas* also (See Fig. 1).

ii. Standard for the cross-sectional brain image planes and sizes

For the sake of convenience, we have presented the images of the reference brain, as well as of the MRI brain in our atlas, on a scale of 1:1. In other words, both cadaver and MRI images are in the actual metric base frames and systems, except the expanded images. The average shrinkage of the cerebral hemisphere resulting from freezing is known to be approximately 1%; therefore, shrinkage due to this reason may be neglected. For the convenience of the readers, we have displayed a few selected images with expanded views to facilitate the visualization of image details. We believe that these magnified images provide relevant information that was previously unavailable.

Extracerebral reference lines have been generally used in radiography, CT, and MRI studies. In 1962, the World Federation of Radiology defined Reid’s base line as the line between the infraorbital margin and the upper margin of the external auditory meatus. In radiological practice, however, the canthomeatal line has been used with a greater frequency than Reid’s base line. The canthomeatal line is the line between the lateral canthus and the central point of the external auditory meatus. The line is pitched at approximately 10° nose-up relative to Reid’s base line, which is approximately parallel to the

"true" horizontal line. However, intracerebral reference points have not been standardized yet. In stereotactic surgery, the foramen of the Monro-posterior commissure line or the AC–PC line has been used as the reference line. Schaltenbrand et al. and Talairach et al. suggested that the anterior and posterior commissures might be considered to have a constant relationship with the deep cerebral structures. These researchers proposed the line between these two commissures to be the basic reference line.

In our *7.0 Telsa MRI Brain Atlas*, the horizontal plane passing through the central point of the AC and PC of the reference brain is designated as the reference axial plane, defined as the central AC–PC intercommissural line. This differs from the convention used in stereotaxy and functional MRI, where the tangential AC–PC line passes through the superior edge of the AC and the inferior edge of the PC (see Fig. 2).

We have extended the concept of the central AC–PC line to the entire brain. We found that our AC–PC line is easy to define and is independent of the size of the AC and the PC, which varies from 3 to 6 mm and from 2 to 4 mm, respectively. We also found that the central AC–PC line is pitched at approximately parallel to Reid's base line and approximately 10° nose-down relative to the canthomeatal line. This line, in turn, is approximately parallel to the "true" horizontal plane. Therefore, we believe that the central AC-PC line can be used as an intracerebral reference axial line for the anatomical horizontal plan (see Fig. 3). This line is close to the normal position of the head in the living subject.

In our book, as mentioned earlier, we have adopted the Cartesian coordinate system, where the x-axis runs through the midpoint of the intercommissural distance of the central AC–PC line, where $x = 0$. The horizontal plane is defined as an axial plane, i.e., x–y plane, which contains the AC–PC line at the center, with a positive sign denoting axial slices superior to the AC-PC line and a negative sign denoting inferior slices. The y–z plane, which contains the AC–PC line, is defined as the plane at the center of all sagittal planes. Similarly, the planes anterior to the central coronal plane (y=0, x–z plane) are designated with a positive sign, while the planes posterior to the central plane are designated as negative. As implied by the images, the central coronal image is defined as the image plane at the center of the AC–PC line at y=0. In the case of the sagittal images, the slices to the left (-x) of the AC–PC line are labeled as negative, while the planes on the right side (+x) of this line are designated as positive. The longitudinal cerebral fissure in considered to be the point of origin for the midsagittal image. In this book, the axial planes are arranged from superior (+z) to inferior (–z), whereas the coronal planes are arranged from anterior (+y) to posterior (–y). The sagittal planes are arranged from right (+x) to left (–x) (See Figs. 1 and 3).

iii. Adjustment of the MRI brain to the reference brain

In order to easily accommodate the anatomical images of the reference brain with the different sizes of *in vivo* brain images obtained through MRI, we have introduced a "Reference Adjusted Unit (RAU)" measured in millimeters (mm). The RAU number represents the MRI image, which resembles the cadaver images shown as No. X in the book. For example, the thalamus lies at the same RAU for a given MRI and cadaver image; however, the actual mm distance from the midline could be different between the cadaver image and the MR image.

The actual lengths in mm from the reference points are shown in every slice of MRI image provided in this atlas. Their measurements are shown in mm values in parenthesis immediately after the RAU number.

For instance, “Axial-MRI: No.+62 (+66 mm)” means that “an axial MR image is located at a position 66 mm superior to the reference axial plane (AC–PC plane), which also corresponds to the cadaver (reference) brain image located at a position 62 mm superior to the reference axial plane designated by “No.+62.” A similar compensation technique is applied to individual variations, both along the coronal and sagittal planes.

iv. Terminology and labeling

Different authors refer to the same brain structures with different names. In this atlas, in an attempt to use the most up-to-date anatomical terminology, we have adopted the standard terms used in “Terminologia Anatomica” by the International Federation of Associations of Anatomists published in 1998. It supersedes the previous standards described in “Nomina Anatomica.”

Many commonly used positional and directional notations are abbreviated. For example, ant. is the abbreviation for anterior, post. for posterior, sup. for superior, inf. for inferior, lat. for lateral, med. for medial, int. for internal, and ext. for external.

All identifiable anatomical structures were labeled on the images of both the cadaver brain and the MRI brain. Because of the structural differences between the right and the left hemisphere, the important structures were labeled on both sides. The cerebral gyri were generally labeled at the white matter core, rather than at the cortical surface. In the brainstem, the major nuclei and tracts have been labeled in the expanded views. We have also divided all the brain sections into major anatomical compartments, i.e., frontal lobe, temporal lobe, parietal lobe, occipital lobe, brainstem, and cerebellum, and also depicted laterality, such as right (R) and left (L). Structures that appeared more than once were designated with numbers (not applied in the case of expanded images).

v. Data collection system for clinicopathologic brain mapping

If a clinicopathological map of the human brain was available, it would serve as a useful supplementary source of information for clinical diagnosis by neuroradiologists, as well as for neuroscience researchers. We have to admit, however, that such a clinicopathological brain mapping can be established only by collecting massive amounts of data scattered around the world from clinicians, particularly radiologists, who routinely perform MRI. Through the collaboration and dedicated support of radiologists and clinicians, we may be able to establish a valuable database that could benefit everyone associated with this field.

For instance, a focal lesion of any size could be traced via the image numbering system presented in this Brain Atlas. First, all MR images should be acquired on the basis of the *x*, *y*, *z*-axes at the mid point (0,0,0) of the AC and PC, so that the coordinates of those images are consistent with the Cartesian coordinates of the corresponding images provided in this atlas. Subsequently, images are normalized to our *7.0 Telsa MRI Brain Atlas*. The location of a pathological finding could then be a determined by simply using the grid system consisting of coronal (y), sagittal (x), and axial (z) section lines (Fig. 3). The target point obtained thus would then be indicated as a single dot, or as the midpoint of a target area, thereby identifying the lesion, in 3D. For instance, C(y) –10, S(x) +28, A(z) –20, indicates a point 20 mm inferior to the AC–PC plane along the axial plane, 10 mm posterior to the midpoint of the AC–PC line along the coronal plane, and 28 mm right of the midsagittal plane at the sagittal level. This 3-D location of the lesion would be reported to the National Research Initiative (NRI) center with pertinent neurological findings, together with the identity of the patient. (See Figs. 4 and 5, for examples.)

vi. Figures

Fig. 1 *Views and directions of the brain image*

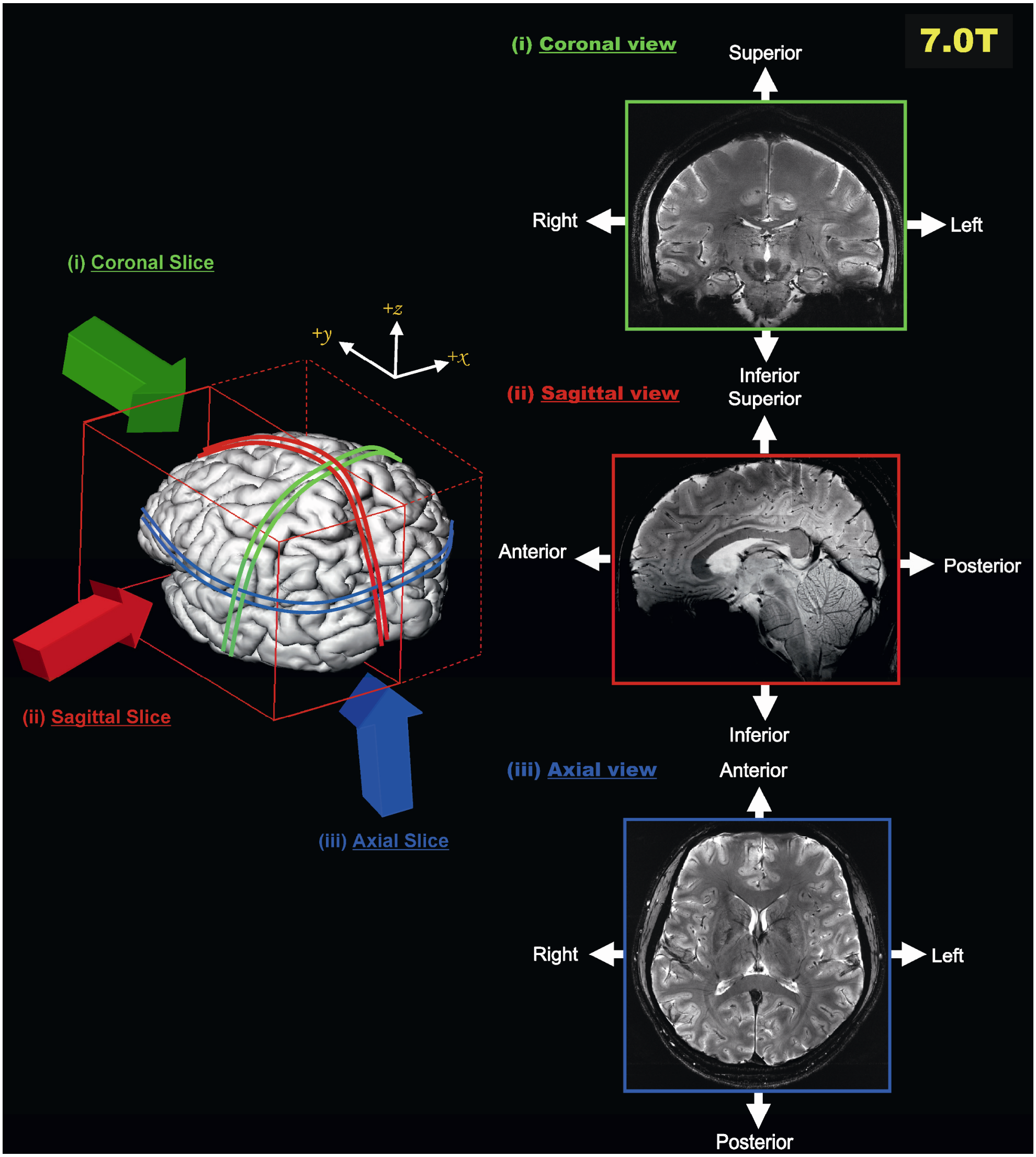

Fig. 2 *Definition of central intercommissural line (central AC–PC line)*

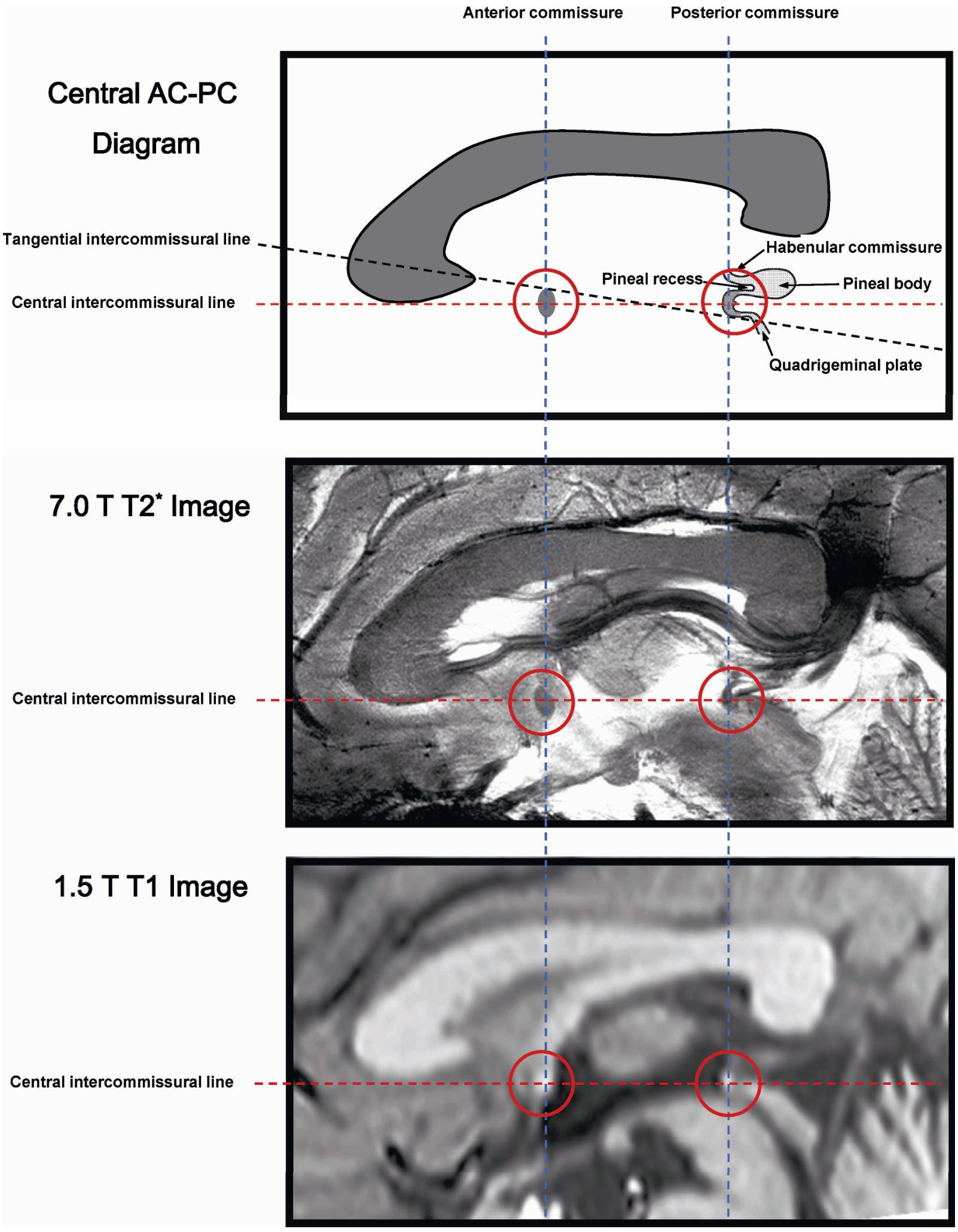

Fig. 3 *Standardization and data set*

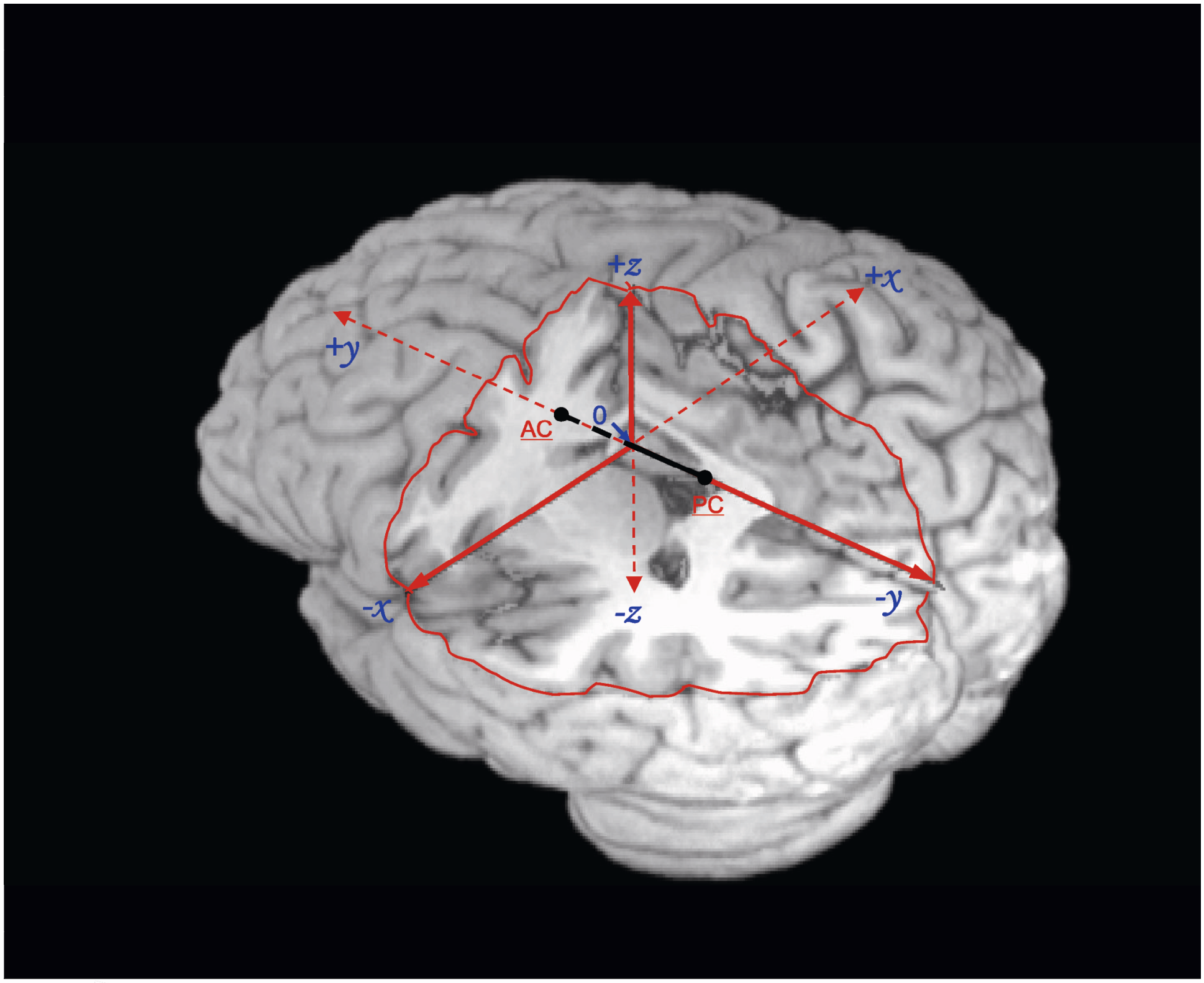

Coronal (y)	Anterior to the center of AC-PC line	+y (+)
	Posterior to the center of AC-PC line	-y (-)
Sagittal (x)	Right of AC-PC line	+x (+)
	Left of AC-PC line	-x (-)
Axial (z)	Superior to the AC-PC line	+z (+)
	Inferior to the AC-PC line	-z (-)

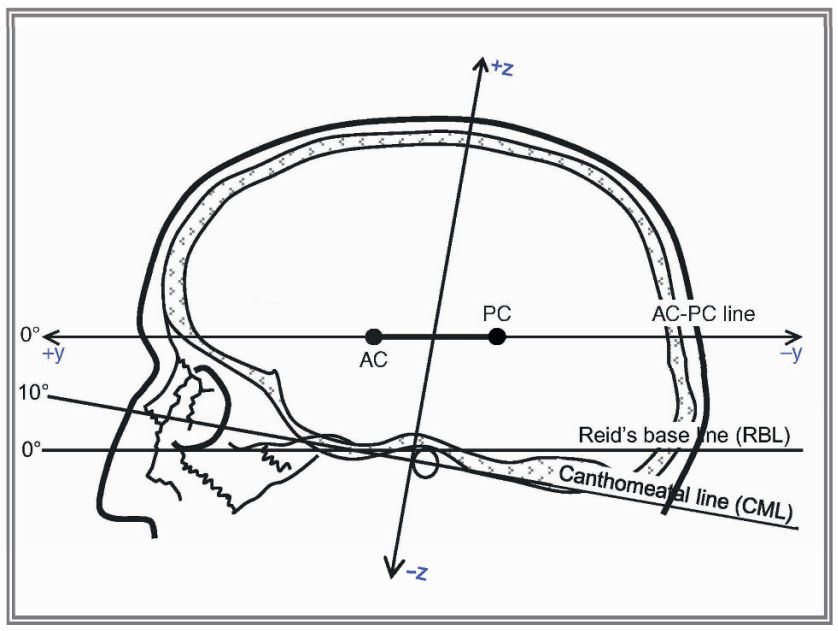

Fig. 4 *Data collection system for Clinicopathologic Brain Mapping (CBM)*

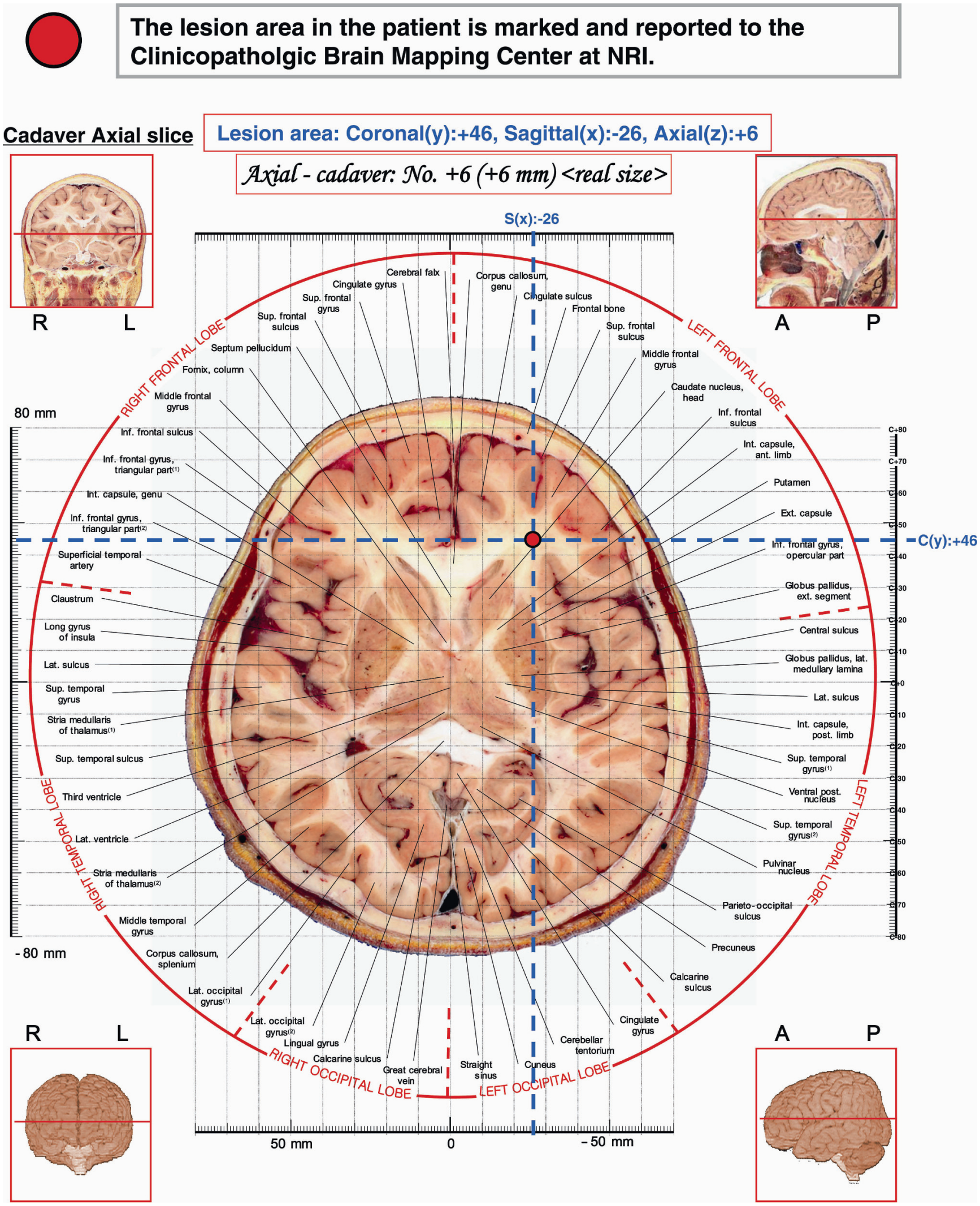

Through the collaboration and enthusiasm of radiologists, neurologists, and neurosurgeons around the world, we might be able to establish a meaningful database that everybody in the neuroscience field would benefit from.

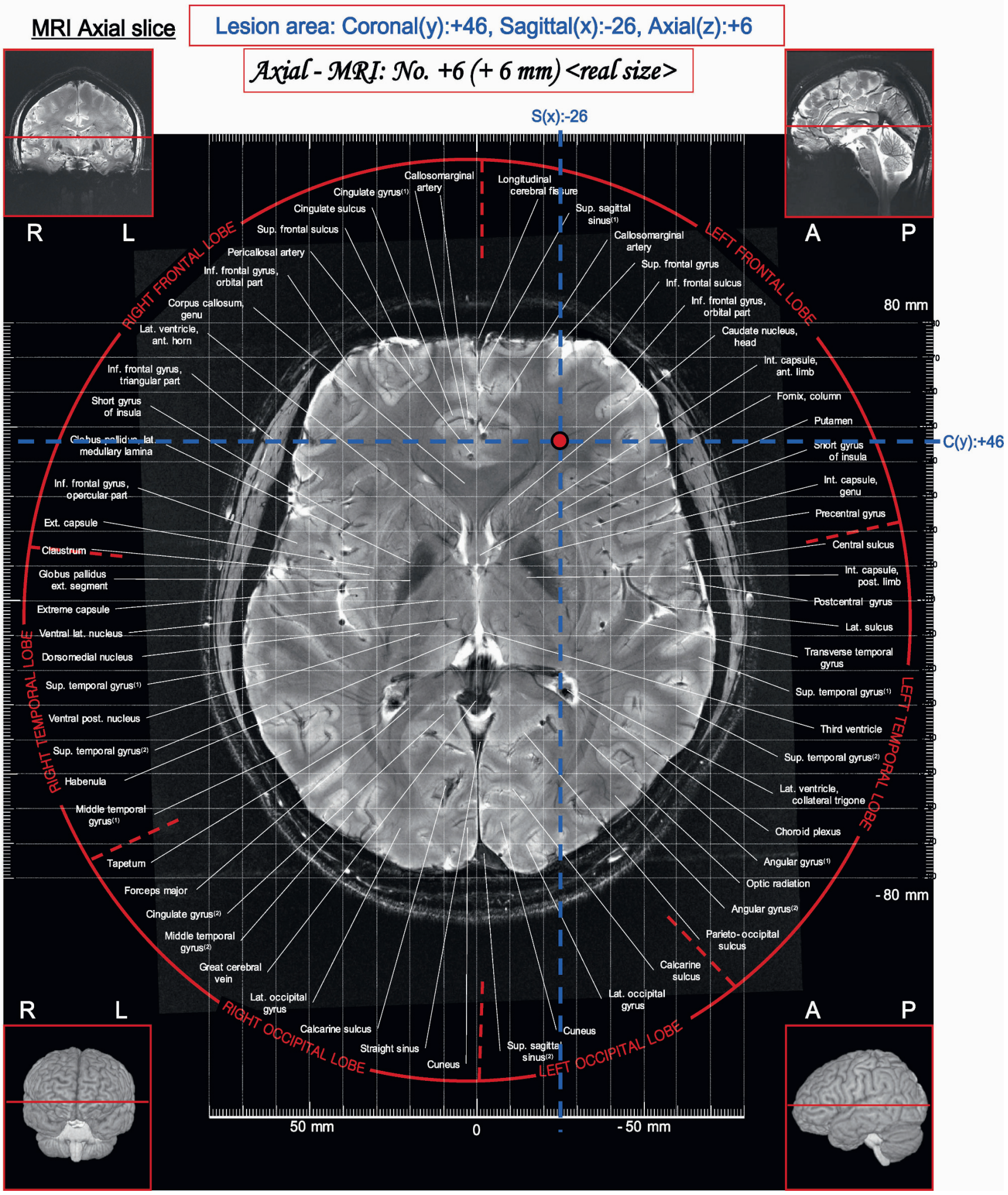

Fig. 5 *Example of Clinicopatholgic Brain Mapping (CBM) case*

CBM form

Patient ID	00000001	Date	2008.01.19	
Name	C.S.S	Age	Sex	Race
		70	F	Asian
Patient's complaint	Headache of 2 years duration			
Neurological findings	No abnormal findings on detailed neurological and neuropsychological examinations			
Clinical diagnosis	Brain tumor			
Histopathologic diagnosis	Glioblastoma			

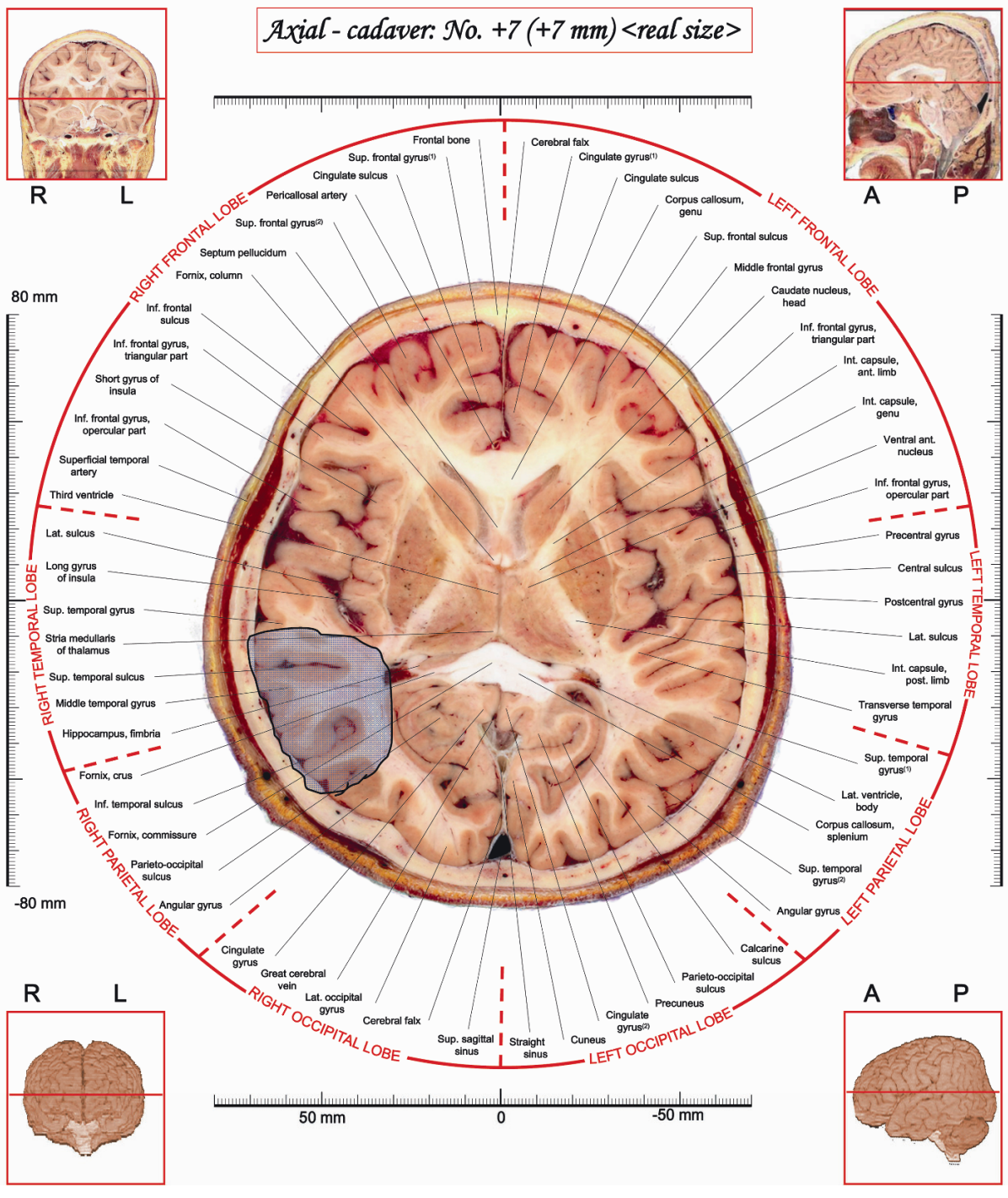

The lesion area seen in the patient's 1.5 T MR image. This area could be mapped using *7.0 Telsa MRI Brain Atlas* coordinates and then reported to the Clinicopathologic Brain Mapping Center at NRI. http://nri.gachon.ac.kr

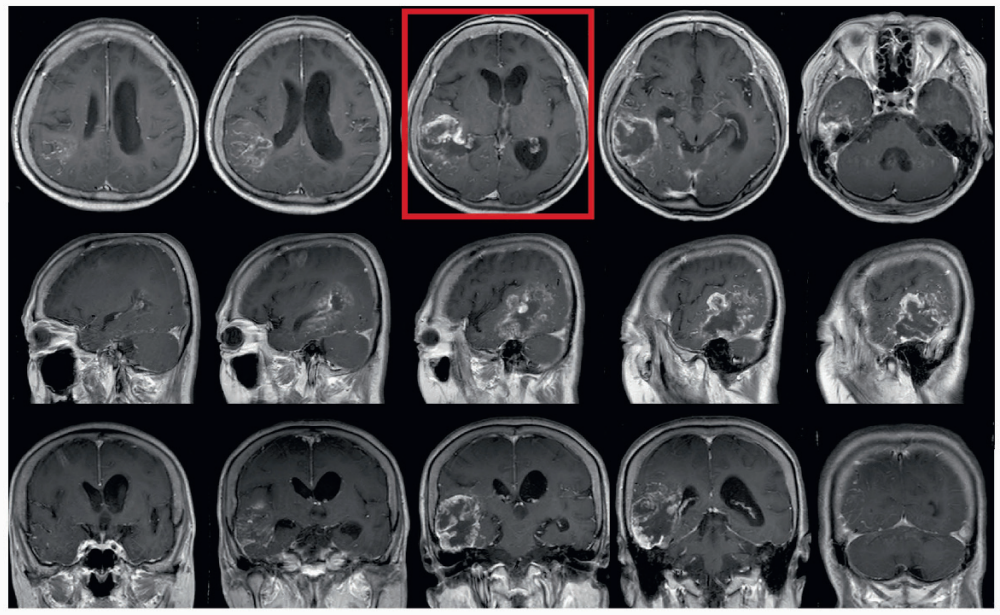

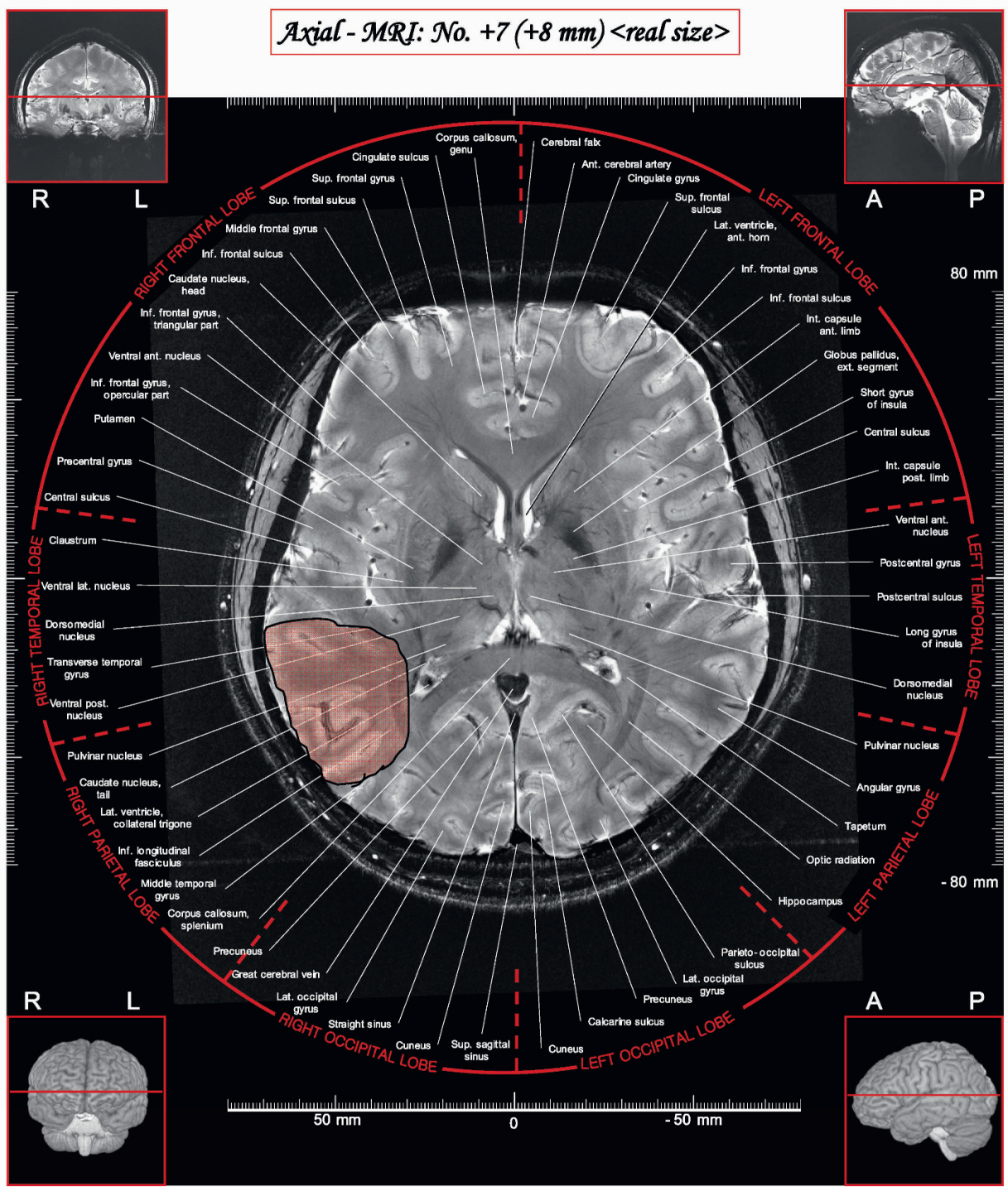

3. Sources of the Brain Images

i. *In vivo images Using 7.0 T MRI*

MRI : 7.0T Research Prototype MRI at the NRI, Gachon University of Medicine & Science
Volunteer: M, 27Y
Axial : No.+62 (+66mm) ~ No. – 58 (– 64 mm): 2 mm interval, Central AC–PC line is set as 0 mm
Sagittal : No.+60 (+65mm) ~ No. – 60 (– 65 mm): 2 mm interval, Center is set at the longitudinal cerebral fissure
Coronal : No.+64 (+66mm) ~ No. – 72 (– 80 mm): 2 mm interval, Midpoint of AC–PC line is set as 0 mm

Our prototype MRI consists of a Siemens Magnetom 7.0 T with a Siemens Avanto series console and electronics. The 7.0 T MRI gradient coil consists of a water-cooled gradient with a field strength of 40 mT/m (4 Gauss/cm). All images were acquired using a conventional 2D Gradient Echo (GRE) sequence. The specific MRI parameters used were repetition time (TR) of 750 msec; echo time (TE) of 17.8 msec; flip angle of 45°; total number of slices per acquisition time (TA) of 12.50 min (or 6.30 min with a reduction factor of 2 in SENSE mode); and bandwidth (BW) of 30. The in-plane resolution was 0.25 mm, with a slice thickness of 2 mm. Cardiac gating was used to minimize pulsation artifacts during *in vivo* human brain imaging. The non-uniformity of the whole brain imaging was then corrected during post processing.

We used a specifically designed 7.0 T brain-optimized SENSE coil (200 mm long and 300 mm in diameter), which covers the entire brain. Our design features include the elongation of the coil to cover the entire brain, especially the lower portion, and the incorporation of multiple symmetric loop coils to encompass the entire brain from the top of the brain to the lower part of the brain in a crown-like shape.

Among many candidates, we selected the image set of a 27-year-old healthy male volunteer. The legal and ethical aspects of the experiments performed for this study were reviewed and approved by the institutional review board (IRB) as well as the government authority, the Korean Food and Drug Administration (KFDA).

ii. *Cadaver images by Cryomacrotome*

Cryomacrotome : Cryomacrotome designed and developed at Ajou University
Volunteer : M, 67Y
Axial : No.+62 (+62mm) ~ No. – 58 (−58mm): 2 mm interval, Central AC–PC line is set as 0 mm
Sagittal : No.+60 (+60mm) ~ No. – 60 (– 60mm): 2 mm interval, Center is set at the longitudinal cerebral fissure
Coronal : No.+64 (+64mm) ~ No. – 72 (– 72mm): 2 mm interval, Midpoint of AC–PC line is set as 0 mm

The cadaver used for this atlas is that of a 67-year-old male, 162 cm tall, weighing 45 kg, who died of cardiorespiratory arrest. He was known to have myasthenia gravis, for which he had been treated for the last several years. He experienced several bouts of an acute upper respiratory infection prior to his death.

His body was first brought to the MRI machine to get a precise axial line along the anterior commissure and posterior commissure, and a sagittal line along the longitudinal cerebral fissure. The axial and sagittal lines were marked with laser indicators. After wards the cadaver was frozen to −70° C for 7 days. The head, together with the upper chest were separated from the main body. The head block was placed into a specially made rectangular frame and frozen again slowly together with embedding media.

The head block was serially sectioned to a 0.1 mm thickness using a cryomacrotome. The sectioning, the rotating speed of cutting disc, and the advancing speed of the embedding box were adjusted, so that 0.1 mm sectioning at each step was precisely accomplished. The sectioning started from the top of the head and was advanced inferiorly along the horizontal plane to the upper end of the spinal cord. A total of 1,248 sectioned surfaces were made, each of which was photographed by using a digital camera (Canon EOS 5D; 50 mm micro lens) and digitized to produce a digital image with 0.1 mm pixel size.

iii. *Image Reconstruction and Volume Rendering*

Based on the original digital axial image data obtained from the horizontal sectioning of the cadaver, we reconstructed both digital coronal and sagittal images. Image errors, such as misalignment and non-uniformity in brightness, were corrected with image processing techniques.

To verify specific structures of the brain, 3D volume rendering was carried out with both the cadaver images and 7.0 T MRI images (Figs. 6 and 7). We then outlined the axial brain image at every 1 mm interval. The brain images were stacked to produce 3D images that were used for the identification of structures on 3D planes. Rendering of the surface anatomy of the cerebral hemisphere was also carried out on both the cadaver brain and the MRI brain, so that individual gyri and sulci, as well as deep structures, could be identified and matched in all three planes. (In Figs. 8 and 9, only the case of MRI is shown.)

4. 3D Images by Volume Rendering

i. *Cironal, sagittal and axial cuts – Cadaver (Fig .6)*

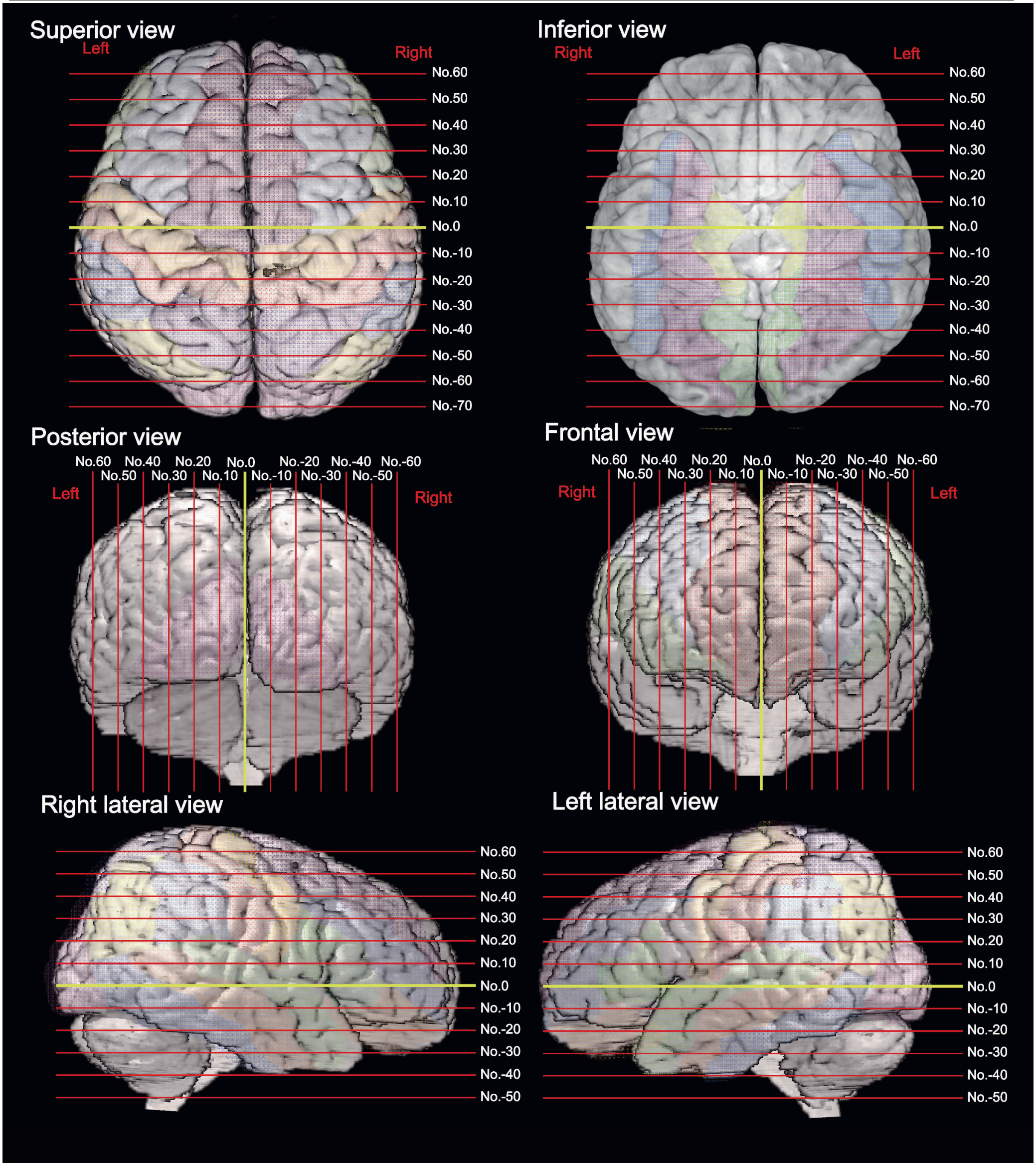

ii. *Coronal, sagittal and axial cuts – MRI (Fig .7)*

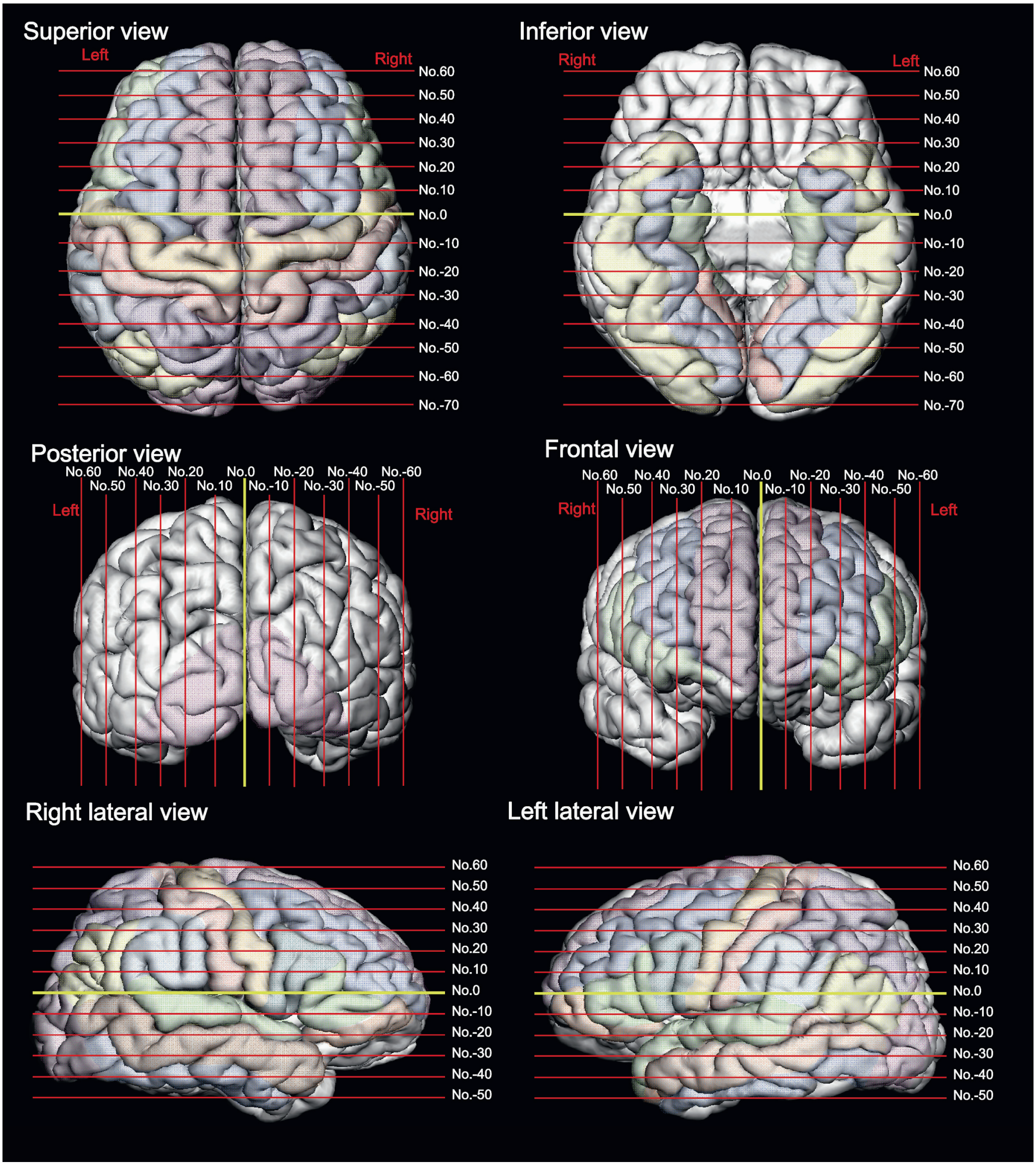

iii. *Sulci and gyri – MRI (Fig .8)*

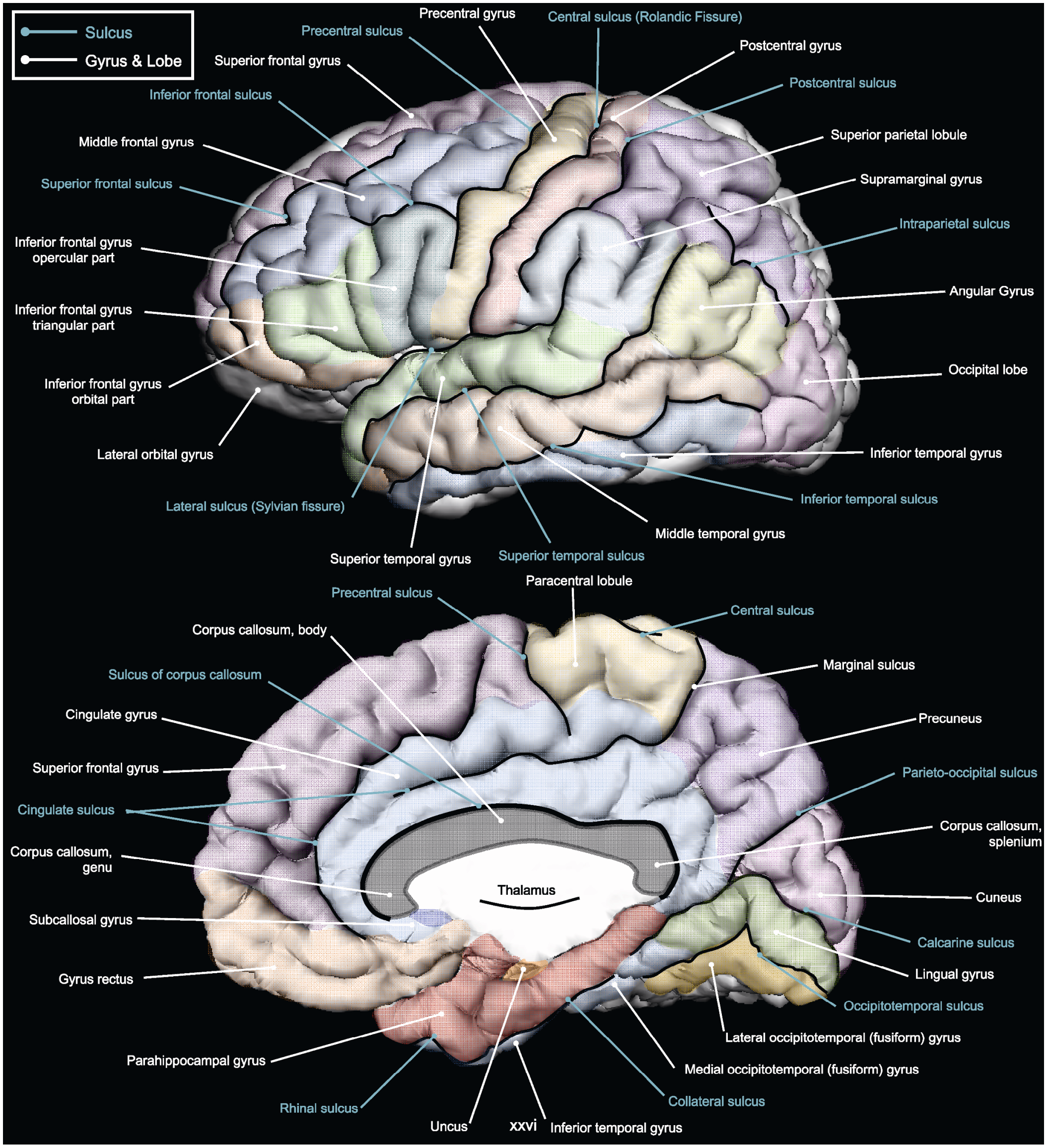

iv. *Brodmann areas – MRI (Fig .9)*

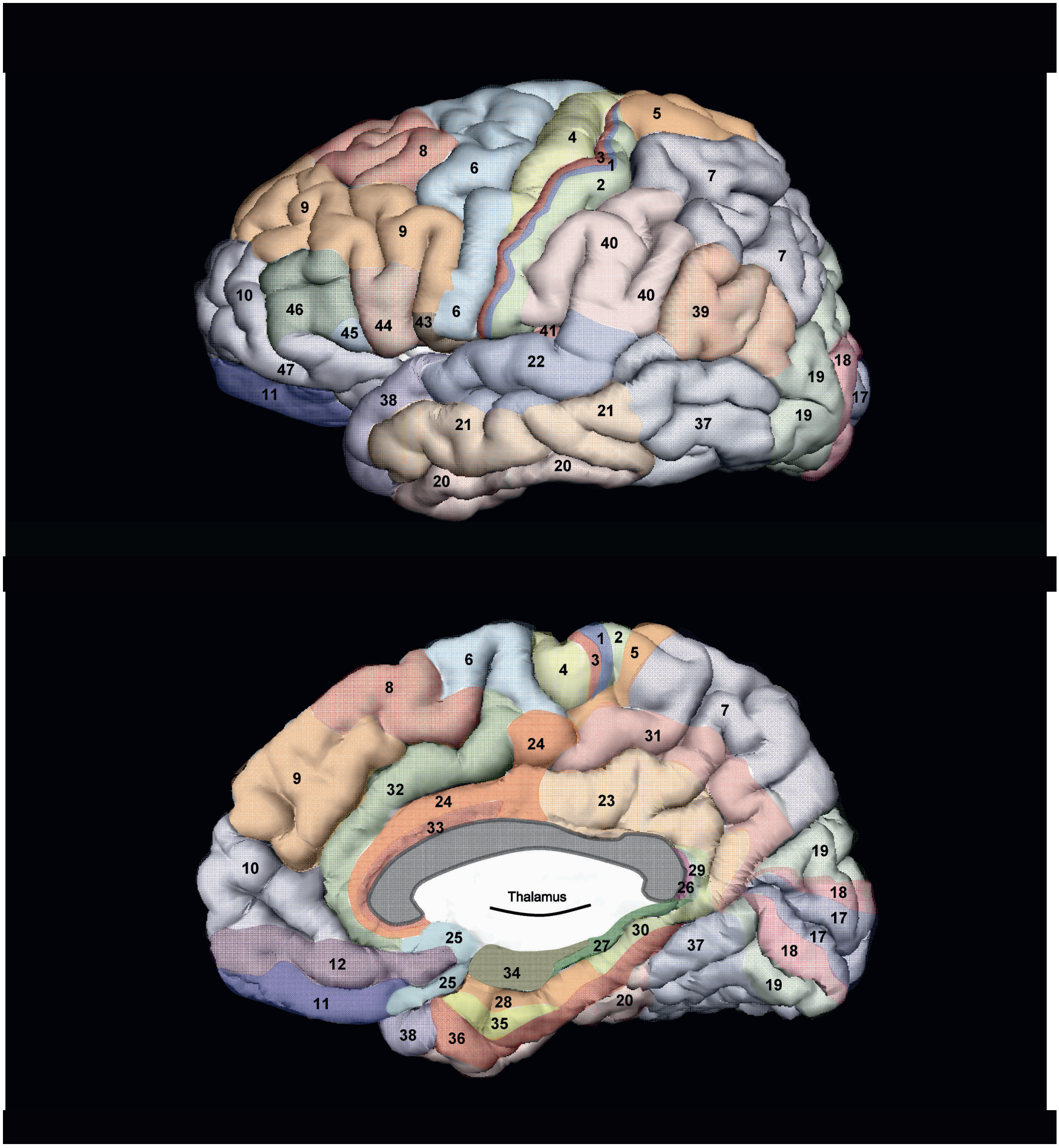

5. Quick Guide to the Use of the 7.0 Tesla MRI Brain Atlas

i. *Notes on the use of the Cadaver images (Fig.10)*

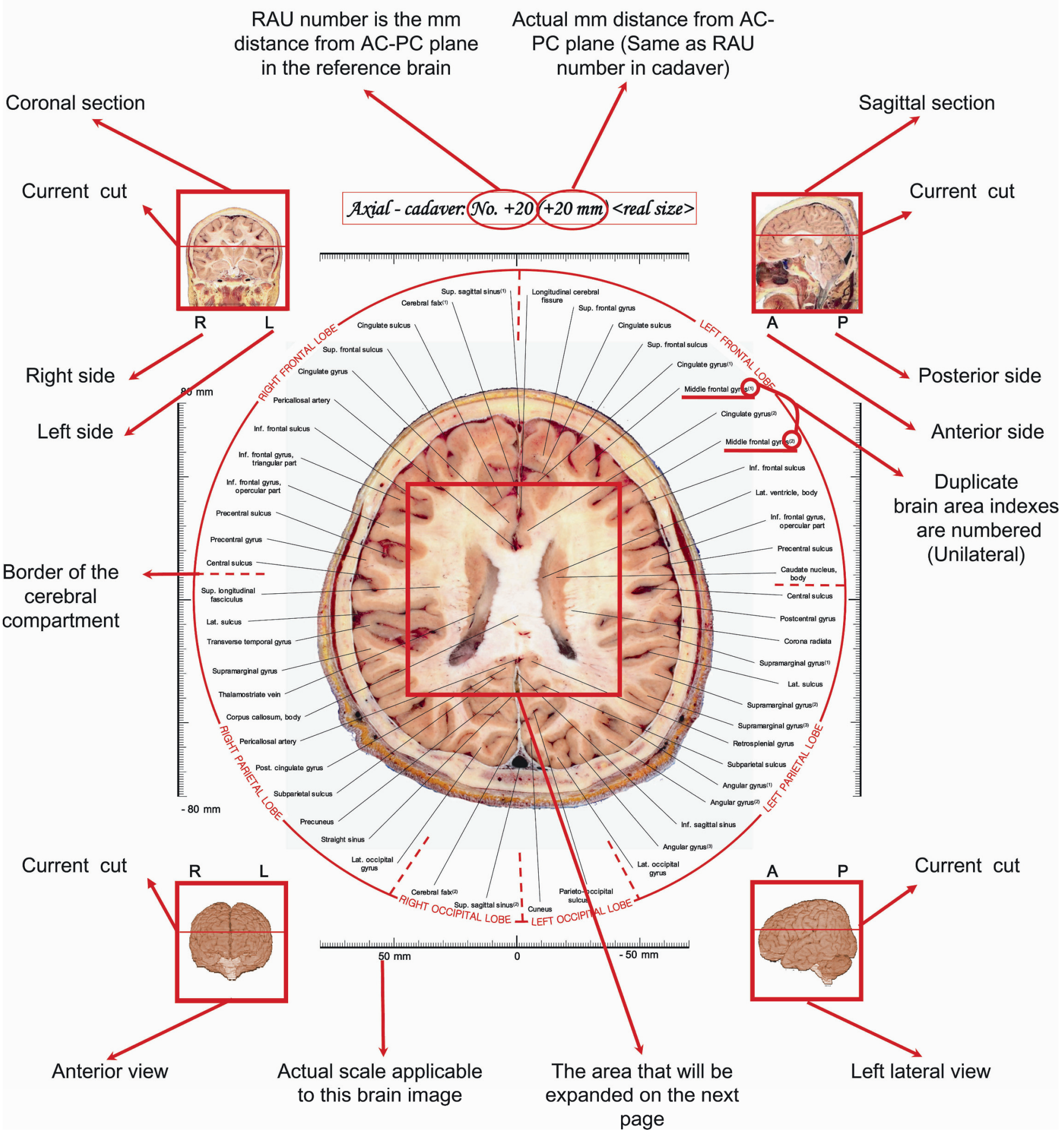

ii. *Notes on the use of the MRI images (Fig .11)*

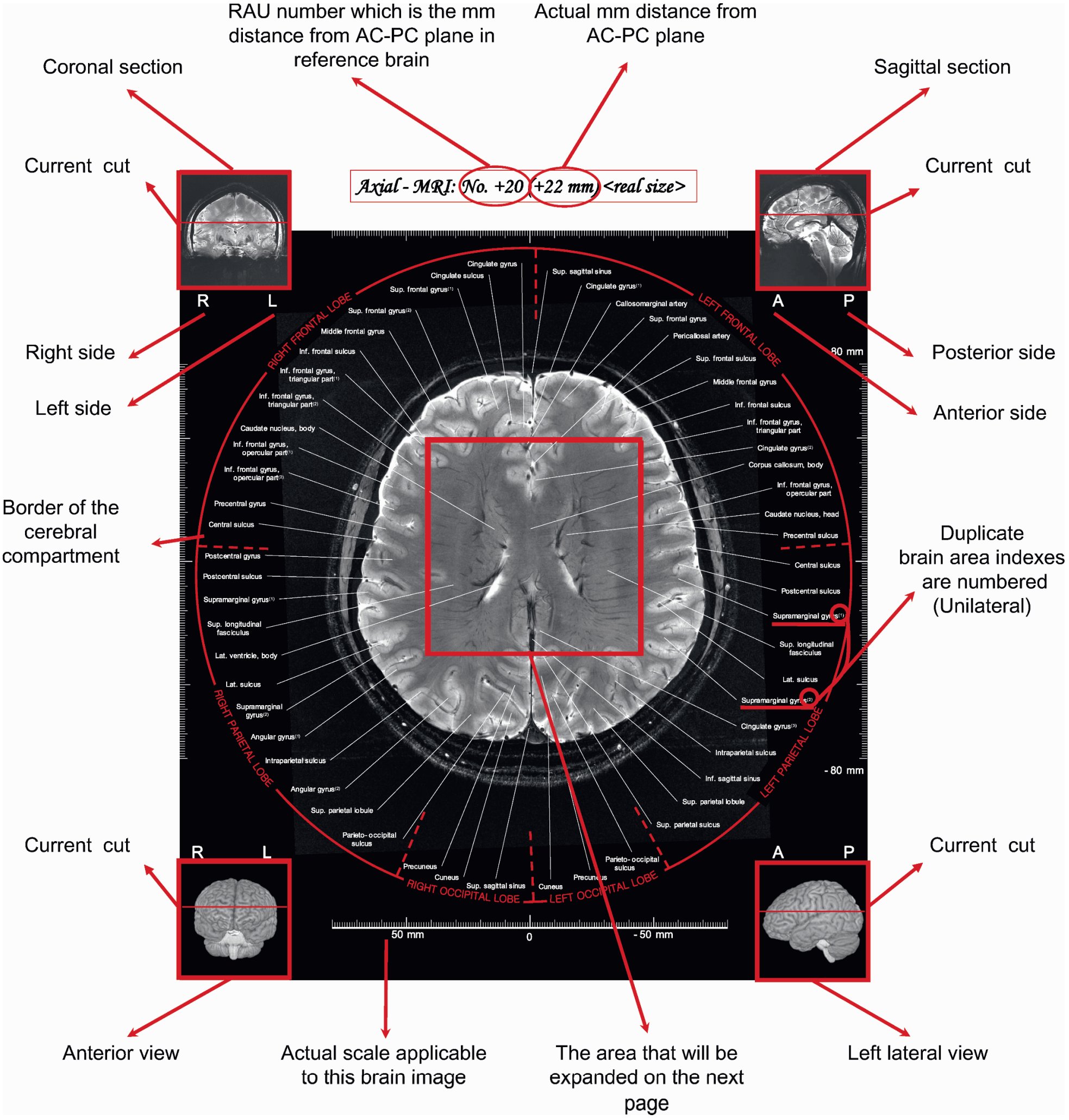

Acknowledgements

This atlas was made possible through the generous support of Dr. Gil-Ya Lee, the Chair woman of the Gil Foundation, whose vision was instrumental in establishing and supporting the Neuroscience Research Institute (NRI). All staff members of the NRI have enjoyed and appreciated the opportunity to work at one of the most advanced research facilities in the world. Thanks are also due to Dr. Chul–Ock Lee, a former adviser to the NRI, whose enthusiasm, commitment, dedication and support made the NRI what it is now. We also like to thanks Siemens as well as their technical staffs who helped us make the 7.0 T system work and function. Without their help it could have not been possible to obtain the fine images seen in this book.

The authors and collaborators are indebted to a large number of individuals, both within and outside the NRI, who greatly contributed to this project. Due to space limitations, it is impossible to list them all, but we are grateful to all of them. The following individuals deserve our special gratitude.

First, we would like to express our gratitude and respect to the cadaver donor and his family for granting permission to use his body for medical research and education, and to the volunteer, who allowed us to procure his MRI images.

We would like to thank all members of the NRI who worked on this project, including the students who helped create the brain maps and improve their appearance: So–Hee Lee, B.A., Myung–Ho In, M.Sc., Nam–Bum Kim, M.Sc., Sung–Tae Kim, M.Sc., Chan–A Park, B.A., Jung–Hwan Kim, B.A., Seok–Il Hwang, B.A., Sung–Yeon Park, B.A. and Hyon Lee, MD., Keum–Hwan Ryu, B.A, Without their efforts, this project could not be accomplished.

We would like to thank the Departments of Anatomy of Seoul National University and Catholic University for letting us review cadaver brains to verify the consistency of the AC–PC plane. Thanks also to Dr. Kyu–Chang Wang, Professor of Neurosurgery at the Seoul National University College of Medicine for his advice in formulating the reference adjustment. We would like to thank Dr. Kun–Sang Kim, Professor of Radiology at Chung–Ang University College of Medicine, Dr. Dong–Ik Kim, Professor of Neuroradiology at Yonsei University College of Medicine, Dr. Gham Hur, Professor of Radiology at Inje University Ilsan Paik Hospital, and Dr. In One Kim, Professor of Radiology at Seoul National University Children's Hospital for their advice in formulating the reference planes.

We would like to thank the Korea Institute of Science and Technology Information for their financial support preparation of the reference brain images. We also appreciate the collaboration of Ki Ho Im, M.Sc. Hanyang University, Hyun Ji Kwon B.A. of Samsung Medical center, and Hong Gyun Park, MD of Yonsei University.